Title	High-precision measurement of an involute artefact by a rolling method and comparison between measuring instruments
Author(s)	Takeoka, Fumi; Komori, Masaharu; Kubo, Aizoh; Fujio, Hiroshige; Ito, Takehiro; Takatsuji, Toshiyuki; Osawa, Sonko; Sato, Osamu; Takeda, Ryohei
Citation	Measurement Science and Technology (2009), 20(4)
Issue Date	2009-02-19
URL	http://hdl.handle.net/2433/210472
Right	This is an author-created, un-copyedited version of an article accepted for publication in 'Measurement Science and Technology'. The publisher is not responsible for any errors or omissions in this version of the manuscript or any version derived from it. The Version of Record is available online at http://dx.doi.org/10.1088/0957-0233/20/4/045105.
Type	Journal Article
Textversion	author

High Precision Measurement of Involute Artefact by Rolling Method and Comparison between Measuring Instruments

Fumi TAKEOKA[1], Masaharu KOMORI[1,4], Aizoh KUBO[1], Hiroshige FUJIO[1], Takehiro ITO[1], Toshiyuki TAKATSUJI[2], Sonko OSAWA[2], Osamu SATO[2] and Ryohei Takeda[3]

1 Department of Mechanical Engineering and Science, Kyoto University, Yoshidahonmachi, Sakyo-ku, Kyoto-shi, Kyoto 606-8501, Japan

Tel: 81-75-753-5858

Fax: 81-75-753-5858

E-mail: komorim@me.kyoto-u.ac.jp

2 Dimensional Standards Section, National Metrology Institute of Japan, AIST, Tsukuba, Ibaraki 305-8568, Japan

Tel: 81-29-861-4361

Fax: 81-29-862-6045

E-mail: toshiyuki.takatsuji@aist.go.jp

3 Engineering Division of OSAKA SEIMITSU KIKAI Co., Ltd., 6-5-16 Mikuriya, Higashioosaka-shi, Osaka 577-0032, Japan

Tel: 81-6-6782-0648

Fax: 81-6-6782-0448

E-mail: r-takeda@osk-corp.co.jp

4 Corresponding author

Abstract. The vibration of gears is one of the serious problems for machines. The characteristics of vibration of gears are affected by tooth flank form deviation of submicrometer order. The quality of product gears is controlled by a gear-measuring instrument, which is calibrated by an involute artefact with high precision. A highly precise method of measuring the involute artefact by rolling has been proposed. However, this method does not yield sufficient accuracy. In this research, a novel rolling method for the involute artefact, "nonslip driving method", is proposed to achieve high accuracy. This method is compared with the conventional driving method by theoretical analysis of artefact motion. Moreover, its accuracy and effect are evaluated experimentally. The results show that this method is more stable on the basis of measurement results than the conventional driving method. Therefore, it is confirmed that the highly precise measurement of the involute artefact can be realized by incorporating the nonslip driving method into the rolling artefact method. In addition, measurement results for the involute artefact are compared among the proposed method and the methods involving the use of a coordinate measuring machine and a gear-measuring instrument.

Keywords: gear, involute, artefact, measurement, rolling, laser interferometer

1. Introduction

Reducing the levels of vibration and noise is one of the serious challenges for involute spur and helical gears used for the drivetrain of vehicles, such as automobiles. Studies on gear vibrations have been carried out [1]. A gear tooth flank form of submicrometer order markedly affects gear vibration and noise; therefore, the strict quality control of the tooth flank form must be performed to realize excellent gear performance. A gear is inspected using a gear-measuring instrument, and to calibrate it, an artefact with high accuracy is used. Studies on the accuracy assessment of the gear-measuring instrument have been performed [2,3] and various artefacts for inspecting the gear-measuring instrument have been proposed [4-6]. In realizing excellent quality control, highly precise and traceable calibrating technology for the artefact is one of the most important factors [4,7]. An involute artefact is used to calibrate the gear-measuring instrument for profile form measurement. The involute artefact is typically calibrated using a highly calibrated coordinate measuring machine or a calibrated gear-measuring instrument [8]. Recently, studies on a novel calibration method for the artefact have been reported. For example, Haertig and coworkers have developed a measuring method incorporating the coordinate measuring machine with a tracking laser interferometer [9,10].

Mintrop and Beyer have developed a highly precise method of measuring an involute artefact [11]. This method is called the “rolling artefact method” in this report. In this measuring method, the involute artefact is rolled and its form is measured by fixed displacement sensors, where the geometric feature of the involute curve is applied. The rolling artefact method is known as the highly accurate measuring method. We have proposed a measuring method based on the rolling artefact method, in which displacement is directly measured using a laser interferometer [12]. In Mintrop and Beyer’s and our measuring methods, an involute artefact with base cylinders is rolled horizontally during measurement. Thus, the accuracy of rolling motion of the involute artefact directly affects the measurement accuracy. Therefore, the rolling motion accuracy must be increased to realize a more accurate measurement.

In this research, to achieve a more accurate rolling motion of the involute artefact, a nonslip driving method is proposed, in which the involute artefact rolls horizontally without slippage. This method is compared with the conventional driving method by theoretical analysis of artefact motion. These driving methods are also compared experimentally and the efficiency of the proposed method is verified. In addition, the involute artefact is measured using a coordinate measuring machine and a high-precision gear-measuring instrument, and the measurement results are compared among these devices.

2. Measuring device and involute artefact [12]

The bold line in figure 1 shows the base circle and involute curve, which is defined by the base circle that contacts line AB. Suppose that the base circle and involute curve roll as one body on line AB towards the left in figure 1 without slippage between the base circle and line AB, and then reach the position shown by the dotted line in figure 1. During this rolling motion, the involute curve and line AB always perpendicularly intersect at crossing point P, which is a special feature of the involute curve. Conversely, if this curve is not a true involute curve, that is, if it has a form deviation from the involute curve, the position of crossing point P

changes. The displacement of crossing point P in the direction of line AB indicates the profile form deviation. A tooth profile deviation curve is typically expressed as a graph with the profile form deviation on the y-axis and the rolling length of the base circle on the x-axis. Therefore, the tooth profile deviation curve of the involute artefact can be obtained by measuring the displacement of crossing point P while measuring the rolling length of the base circle. We have already proposed the measurement method [12], where the rolling length of the base circle and the displacement of crossing point P are measured by laser interferometry by directly pointing a laser beam to the surface of the involute artefact, as shown on the right side of figure 1. This method using laser interferometry is used in this research.

Figure 2 shows the involute artefact used in this research. It consists of an involute tooth flank section and two base cylinders, which correspond to the base circle of the involute tooth flank. The base cylinders are installed on both sides of the tooth flank section. There are discs between the base cylinders and the tooth flank to protect the tooth flank. The tooth flank is produced in such a way that the base circle radius of its involute curve is 57.5 mm. The designed radius of the nonpolished surface area of each base cylinder is identical to the base circle radius (57.5 mm). The radius and roundness of the unpolished part of the base cylinder are measured using a coordinate measuring machine (Leitz PMM12106) and a roundness measuring machine (Kosaka laboratory corporation roncorder EC3400) at the National Metrology Institute of Japan, respectively. The radius is 57.5010 mm and the roundness is 77 nm on the left base cylinder in figure 2, whereas the radius is 57.5008 mm and the roundness is 82 nm on the right base cylinder, at a temperature of 20 degrees C. The combined standard uncertainty for the radius measurement is 80 nm, and the standard uncertainty for the roundness measurement is 20 nm. The compression of base cylinders due to self weight is evaluated using Finite Element Method. The change of the radius of the base cylinders due to compression is estimated to be 2.35×10^{-7} μm, and its effect on measurement result is negligibly-small.

The involute artefact is set on the rail of the measuring device. The nonpolished surface area of each base cylinder contacts the rail. The artefact is rolled by the driving system described in the next section according to the measurement principle (c.f. figure 1). The rolling length of each base cylinder is measured using laser interference by pointing a He-Ne laser beam to the polished areas (the middle areas) of the two base cylinders. The displacement of the tooth flank is measured by pointing a focus laser beam to the tooth flank of the artefact.

3. Conventional and novel driving systems of involute artefact

3.1. Wound-belt driving system [12]

Beyer of Physikalisch-Technische Bundesanstalt rolls the involute artefact as shown in figure 3, in tooth profile measurement. A wire is wound around the involute artefact and equipment strains the wire. The wire is reeled and released, and the involute artefact rolls on the rail according to the movement of the wire. We have already proposed a simplified driving system, as shown in figure 4, to roll the artefact. One end of the steel belt is fixed to the winding disc (diameter of 145 mm) attached to the stepping motor and the belt is

hung on the protector disc (diameter of 145 mm, c.f. figure 2) of the involute artefact. At the other end of the steel belt, a pedestal (200 g) and a weight (1 kg) are placed. The steel belt is reeled in and out by the rotation of the stepping motor. The stepping motor rotates 0.0072 degrees in one pulse.

3.2. Nonslip driving system

In the rolling artefact method, the slippage between the artefact and the rail of the measuring device affects the accuracy of the measurement. In this report, we propose a new driving system for the involute artefact shown in figure 5 to realize nonslip driving. Figure 6(a) shows the photo of the entire system and figure 6(b) shows its closeup. A rubber belt is tensioned between two pulleys in the horizontal direction, and one pulley is connected to the stepping motor with another rubber belt. The belt between the two pulleys is driven by the rotation of the motor. The involute artefact has a small disc (c.f. figure 2) with a radius of 32 mm. The belt contacts this small disc as shown in figure 6(b), and the involute artefact is driven by the frictional force between the belt and the small disc. Around the contacting area of the belt, another rubber part is attached to the belt to intensify the frictional force.

4. Theoretical analysis of artefact motion and comparison between two driving systems

4.1. Wound-belt driving system

A simplified motion model of the involute artefact rolled by the wound-belt driving system is shown in figure 7. The parameters of the model are the mass of the involute artefact M, the moment of inertia I, the rolling radius of the base cylinder r, the radius of the disc of the involute artefact driven by the belt a, the displacement distance x, the angle of rotation θ, the driving force applied to the disc of the involute artefact by the steel belt F_1, and the frictional force between the artefact and the rail F_2. The frictional force F_1 between the artefact and the belt gives a torque to the involute artefact and this torque causes the frictional force F_2. F_2 moves the involute artefact to the right while preventing the relative slippage between the artefact and the rail. Equations of motion are as follows.

$$M\ddot{x} = F_2 \tag{1}$$

$$I\ddot{\theta} = aF_1 - rF_2 \tag{2}$$

If the translational acceleration $\ddot{x}$ corresponds to the circumferential acceleration $r\ddot{\theta}$, the displacement distance of the center of the base cylinder becomes identical to the contact length of the rail and the surface of the base cylinder; in other words, the slippage between the base cylinder and the rail does not occur. F_2 can be expressed as follows when the acceleration $\ddot{x}$ equals $r\ddot{\theta}$.

$$F_2 = \frac{Mar}{I + Mr^2} F_1 \tag{3}$$

4.2. Nonslip driving system

A simplified model of the nonslip driving system is shown in figure 8. The equations of motion are as follows, where the lateral force applied to the involute artefact by the belt is F_3, the vertical distance between the artefact axis and the line of action of the lateral force is h, and the frictional force between the artefact and the rail is F_4.

$$M\ddot{x} = F_3 + F_4 \tag{4}$$

$$I\ddot{\theta} = F_3 h - F_4 r \tag{5}$$

h is chosen as eq. (6) in this system.

$$h = \frac{I}{Mr} \tag{6}$$

This yields the agreement between the acceleration $\ddot{x}$ due to the lateral force F_3 and the circumferential acceleration $r\ddot{\theta}$ due to the torque $F_3 h$. The initial velocities $\dot{x}$ and $r\dot{\theta}$ are zero because the artefact is stationary at the start of rolling. Therefore, the translational displacement x is equal to the contacting distance $r\theta$ between the artefact and the rail. In other words, the lateral force F_3 causes both the lateral movement and rotation of the involute artefact without causing the relative movement between the base cylinder surface and the rail. Namely, the rolling motion without the slippage between the artefact and the rail can be achieved. As a natural result, the frictional force F_4 does not occur under this condition. h is 32.0 mm for the involute artefact used in this study according to eq. (6). The small disc of the involute artefact (c.f. figure 2), which contacts the belt, has this radius.

4.3. Difference between two driving systems

In the wound-belt driving system, the belt gives a torque to the artefact and the torque rotates the artefact. Under this condition, the frictional force between the artefact and the rail is generated to prevent the slippage. As a result, the frictional force between the artefact and the rail makes the lateral motion of the artefact. On the other hand, in the nonslip driving system, the force given by the belt causes both the lateral motion and rotation. There are no factors that generate the slippage between the artefact and the rail; therefore, the frictional force between the artefact and the rail does not occur. In other words, the wound-belt driving system induces a force to generate the slippage, although the slippage is prevented by the frictional force. The nonslip driving system does not have any factors that generate the slippage. This is the difference between these two driving systems. On the basis of the results of this analysis, the wound-belt driving system accommodates the possibility that the artefact slips on the rail, whereas the nonslip driving system does not. Even if the nonslip driving system is used, it is impossible to thoroughly prevent slippage, and microscopic slippage might occur between the involute artefact and the rail. However, the wound-belt driving system induces a force to generate the slippage, and thus both the macroscopic and microscopic slippages are caused. The effect of the macroscopic slippage is far larger than that of the microscopic slippage, and thus the

nonslip driving system leads to considerable reduction of the effect of the slippage. Therefore, the measurement accuracy is supposed to be higher using the nonslip driving system than using the wound-belt driving system.

5. Experimental comparison between two driving systems

5.1. Effect of measurement direction

The profile of the artefact is measured from root to tip when the artefact is rolled in the direction of the arrow in figure 1. Conversely, the profile is measured from tip to root when the artefact is rolled in the opposite direction.

Figure 9 shows the mean curve of the measured profile deviation curves using the wound-belt driving system. Ten round trip measurements (tip-to-root and root-to-tip) are carried out at a driving frequency of the stepping motor of 100 Hz. The two profile deviation curves exhibit a difference with a maximum of 140 nm.

In root-to-tip measurement, the belt is reeled in by the stepping motor; in other words, the artefact is accelerated by the stepping motor. On the other hand, in tip-to-root measurement, the belt is released, and therefore, the artefact is driven mainly by gravity. In the case that the rotational acceleration of the artefact given by the belt is large, the frictional force between the artefact and the rail cannot prevent the slippage. The acceleration given by the stepping motor is supposed to be larger than the gravity. It is therefore supposed that root-to-tip measurement has a higher probability of slippage than tip-to-root measurement. Suppose that the frictional force F_2 in figure 7 does not always follow the fluctuation of the circumferential force F_1 in root-to-tip measurement. This causes the shorter lateral motion of the artefact than its rotational motion, as shown in figure 10(a). The repetition of this motion causes the more negative inclination of the measured profile deviation curve as shown in figure 10(b). Therefore, the profile deviation curve of root-to-tip measurement has a more negative inclination than that of tip-to-root measurement. The experimental result shown in figure 9 is in good agreement with the result of this analysis.

Figure 11 shows the mean profile deviation curves obtained using the nonslip driving system. The repetition and driving frequency are the same as those in the above-mentioned experiment (c.f. figure 9). The two measurement curves are almost identical. The difference between them is approximately 60 nm. The measurement repeatability is better than the case shown in figure 9. This result indicates that the nonslip driving method is negligibly affected by the measurement direction.

5.2. Effect of driving frequency

The profile deviation curve of the involute artefact has been measured 10 times using the wound-belt driving system from tip to root at different driving frequencies of the stepping motor in the previous study [12]. Measured profile deviation curves at motor driving frequencies of 50, 75 and 100 Hz are shown in figure 12. At the frequency of 100 Hz, high-frequency fluctuation can be observed in the tooth profile curve and the repeatability deteriorates. Figure 13 shows the result of the discrete Fourier transformation of time-varying

profile deviation. A peak can be seen in the high-frequency range at all driving frequencies, indicating the existence of high-frequency vibration. The total profile deviations are calculated for the obtained profile deviation curves according to ISO 1328-1 [12]. The averages and standard deviations of the total profile deviations are plotted as a function of the driving frequency of the motor in figure 14. The average of the total profile deviations of root-to-tip measurement is larger than that of tip-to-root measurement because the former profile deviation curves have a larger inclination than the latter, as shown in figure 9. In figure 14, the tip-to-root measurement result varies largely depending on the driving frequency, and the standard deviation deteriorates at driving frequencies of 50, 100 and 200 Hz where high-frequency fluctuation is observed in the profile deviation curve. On the other hand, root-to-tip measurement is less affected by the difference in driving frequency than tip-to-root measurement. This difference in the effect of driving frequency between tip-to-root and root-to-tip measurements is probably caused by the difference in main acceleration force, that is, that of the stepping motor or gravity.

Using the nonslip driving system, the profile deviation curve of the involute artefact is measured from tip to root 10 times at different driving frequencies of the stepping motor. Measured profile deviation curves are shown in figure 15. The fluctuation of the measured profile deviation curve is very small under each condition compared with that obtained by the wound-belt driving system (c.f. figure 12). Figure 16 shows the result of the discrete Fourier transformation of time-varying profile deviation. Any peak does not exist in the high-frequency range, in contrast to the case of the wound-belt system, as shown in figure 13. The averages and standard deviations of the total profile deviations are plotted as a function of the driving frequency of the motor in figure 17. The dependence of measurement on driving frequency is reduced. The repeatability is improved at almost all frequencies. These results indicate that a more accurate measurement can be achieved by the proposed nonslip driving method.

5.3. Effect of roller position

In the wound-belt driving system, the position of the roller probably affects measurement results. As the broken line in figure 18 shows, tooth profiles are measured at three different positions of the roller. The standard setting position of the roller is position A, position B is 50 mm farther from the motor from position A, and position C is 80 mm closer to the motor from position A. Figure 19 shows the result of the tooth profile measurement. The inclination of the profile deviation curve differs largely depending on the setting position of the roller. As shown in figure 20(a), a lateral force is not applied to the artefact by the belt at roller position A. When the artefact is driven with the belt slanting between the involute artefact and the roller, a lateral force is applied to the involute artefact, as shown in figures 20(b) and (c). When the roller is at position B (c.f. figure 20(b)), a right-oriented force is applied to the artefact and the artefact may slip on the rail in that direction. The effect of the slippage on the measurement result under roller position B is shown in figure 21, where tip-to-root measurement is taken as an example. The amount of slippage Δd is superimposed on the measured displacement of the base cylinder and the measured profile deviation. The range of the displacement of the base cylinder is approximately 30 mm in total; therefore, the minute

slippage is negligible. However, the slippage directly affects the measured profile deviation because the profile deviation is measured at a submicrometer-order level. As shown in figure 21(b), the measured profile deviation curve has a more positive inclination than that without slippage when positive slippage Δd is continually superimposed on the measurement result. Conversely, in the measurement under roller position C, the artefact can slip in the opposite direction. In this case, negative slippage $-\Delta d$ is superimposed continually on the measured profile deviation and the measured profile deviation curve has a more negative inclination. Figure 19 shows that the measured profile deviation curve under roller position B has a more positive inclination, whereas it has a more negative inclination under roller position C. This experimental result is in agreement with the explanation above.

Even if the roller is at the standard setting position (position A), it is supposed that slippage can occur between the artefact and the rail because the belt changes its slanting condition according to the displacement of the artefact during measurement, as shown in figure 22. Consequently, this is the problem of this driving method.

In contrast, in the case of the nonslip driving system, the force applied to the artefact does not change during the measurement because the contact condition between the belt and the artefact is constant. Therefore, the nonslip driving system is stable.

5.4. Effect of weight size

Five repetitive measurements are carried out using the wound-belt driving system under four different weight conditions (c.f. figure 4): 0.0 kg (only pedestal), 0.5 kg, 1.0 kg and 2.0 kg. The standard deviations of the total profile deviations measured under these conditions are 12 nm, 18 nm, 22 nm and 38 nm, respectively. This indicates that the repeatability is better under lighter weight than under larger weight. Figure 23 shows the result of the discrete Fourier transformation of tooth profile deviation expressed as a function of time. The peak near 8.5 Hz is dominant under large-weight conditions. In addition, it was observed that the weight swings with the motion of the belt as shown in figure 24, and the amplitude of the swing is larger under large-weight conditions. These may be the causes of repeatability deterioration under a large weight.

In contrast, the nonslip driving system does not use the weight, and therefore, the effect of the weight does not exist.

5.5. Comparison

In the wound-belt driving system, the measurement result indicates the existence of the slippage. The maximum force F_2 (c.f. figure 7) is limited because it is a frictional force. In this measurement method, the driving force F_1 fluctuates because the steel belt is driven by the stepping motor. Therefore, the frictional force F_2 could not always follow the fluctuation of the circumferential force F_1 due to the limitation of F_2. Under such a condition, minute slippage possibly occurs between the artefact and the rail at each step of the motion. Even if another type of motor, such as a servo motor, is used, the possibility of the slippage remains because of the limitation of F_2. In addition, the wound-belt driving system has problems about the position of

the roller and the weight size.

On the other hand, in the nonslip driving system, slippage does not exist theoretically and the measurement result confirms it. The nonslip driving system is advantageous compared with the wound-belt driving system.

6. Comparison of measurement results between measuring instruments

In the previous chapter, it is found that the repeatability of measurement by the nonslip driving system is high. In this chapter, the involute artefact is measured using a well-calibrated coordinate measuring machine and a gear-measuring instrument, and measured profile deviation curves are compared.

6.1. Measurement using coordinate measuring machine

The involute artefact is measured using a well-calibrated coordinate measuring machine (Leitz PMM12106) at the National Metrology Institute of Japan. Figure 25 shows the setup of the involute artefact on the coordinate measuring machine. The involute artefact is supported by the V-block at the base cylinders. To investigate the effect of the posture of the involute artefact, the involute artefact is measured at four postures, where the direction of the axis of the artefact differs by 90 degrees, as shown in figure 26. Figure 27(a) shows the measured points on the involute tooth flank and base cylinders. To estimate the axis of the involute artefact, the surfaces of the base cylinders of the involute artefact are measured. Five points are measured at every 45 degrees in the upper half on each cross section, as shown in figure 27(b), and obtained coordinates are fitted into a cylinder using a least-squares method. The centre axis of the bestfit cylinder is regarded to be the axis of the involute artefact. The centre line of the tooth flank in the tooth width direction is measured, as shown in figure 27(c). The reference involute is derived using the axis of the involute artefact and the centre point on the measured line. The involute tooth flank is measured from the normal direction of the reference involute.

Figure 28(a) shows the profile deviation curve measured at four postures in the coordinate measuring machine. The measurement results are almost identical but seemed to largely differ around the root. The involute have a small curvature radius around the root and the geometrical errors of the coordinate measuring machine could affect the measurement result much. The difference between the measured curves around the root is about 300 nm, and therefore, the measurement of the involute artefact using the coordinate measuring machine is difficult in root measurement. The expanded uncertainty (coverage factor k=2) for the tooth profile measurement of the involute artefact using a coordinate measuring machine is 500 nm, and the maximum difference between the measured curves is within the range of the uncertainty.

It is supposed that the systematic errors from the probing system and the mechanical system are eliminated by averaging the measurement results at four postures. The mean curve of the profile deviation curves is shown in figure 28(b). For comparison, the result obtained by the nonslip rolling artefact method (the rolling artefact method using the nonslip driving method) is also shown. The difference between the two curves is approximately several tens of nanometers except for the area around the root. This confirms that the measurement result obtained using the nonslip rolling artefact method is in accordance with that obtained

using the well-calibrated coordinate measuring machine. Around the root, a difference of 300 nm is observed between the two curves. One of the reasons for this could be that the coordinate measuring machine has difficulty in the measurement around the root, as described above.

6.2. Measurement using gear-measuring instrument

The involute artefact is measured using High Precision Gear Measuring Instrument at OSAKA SEIMITSU KIKAI Co., Ltd. In the profile measurement, the contact stylus moves in the tangential direction of the base circle synchronizing with the rotation of the measured gear so that the probe follows the theoretical involute. The output of the displacement sensor of the probe directly indicates the tooth profile deviation.

The photo of High Precision Gear Measuring Instrument is shown in figure 29. Figure 30 shows the profile deviation curve measured using the gear-measuring instrument and that measured using the nonslip rolling artefact method. The expanded uncertainty (coverage factor k=2) for the tooth profile measurement of the involute artefact using this gear-measuring instrument is 900 nm as the total profile deviation, and the maximum difference between the measured curves is within the range of the uncertainty. Even around the root, the two curves are almost identical and their difference is negligible.

The experimental comparison between measuring instruments indicates that the proposed measuring method using the nonslip driving system has an excellent accuracy.

7. Conclusion

To measure the involute artefact by the rolling artefact method with high accuracy, a novel driving method for the involute artefact, “nonslip driving method”, is proposed and developed. In this method, the relative motion does not occur at the contacting point between the base cylinder and the rail. This method is compared with a conventional driving method, “wound-belt driving method”, by theoretical analysis of artefact motion. In addition, by incorporating the proposed driving method and laser interferometric measuring system, the accuracy and effect of the driving method are evaluated experimentally. In addition, measurement results for the involute artefact are compared among the proposed method and the methods involving the use of a coordinate measuring machine and a gear-measuring instrument. The following results were obtained.

(1) It was theoretically explained that the slippage between the artefact and the rail can occur when the artefact is driven by the wound-belt driving system. The lateral motion of the involute artefact is caused by the frictional force between the artefact and the rail, and therefore, it is impossible to avoid the slippage. In contrast, in the nonslip driving method, the lateral force given by the belt causes both the lateral movement and rotation of the involute artefact, and therefore, it does not cause the slippage.

(2) The experimental results showed that the measurement direction, the driving frequency of the stepping motor, the position of the roller and the weight affect the measurement result when the wound-belt driving system is used. The effects of these measurement conditions are negligible when the nonslip driving system is used. This indicates that the nonslip driving system is advantageous over the wound-belt driving system.

(3) To validate the nonslip rolling artefact method, the tooth flank form of the involute artefact was measured using a coordinate measuring machine and a gear-measuring instrument for comparison. The measurement results obtained using these measuring instruments are in good agreement with that obtained using the nonslip rolling artefact method. The efficiency of the nonslip rolling artefact method in measuring the involute artefact with high accuracy was confirmed.

Acknowledgements

This research was funded by a Grant-in-Aid for Creative Scientific Research (B).

References

[1] Xianfeng F and Ming J Z 2008 Machine fault feature extraction based on intrinsic mode functions *Measurement Science and Technology* **19**(4) pp.045105

[2] Beyer W 1996 Traceable Calibration of Master Gears at PTB *Technical Paper of American Gear Manufacturers Association(Alexandria)* 96FTM04

[3] Beyer W and Pahl W 1996 Advanced Strategies for the Traceable Calibration of Cylindrical Gears and Bebel Gears at PTB *VDI Berichte* NR 1230 pp. 937-945

[4] Oguma T and Kawasaki Y 2001 History and Prospect of Gear Measuring Instrument Proc. of MPT 2001 *The JSME International Conf. on Motion and Trasmissions (Fukuoka)* pp.623-629

[5] Sammartinia M P and De Chiffre L 2000 Development and Validation of a New Reference Cylindrical Gear for Pitch Measurement *Precision Eng.* **24**(4) pp.302-309

[6] Hartig F, Krystek M and Klein S 2007 Reliable Detection of Periodic Micro Structure on Open Surface *Proc. of ISMTII 2007 (Sendai)* pp.123-126

[7] Och R 2006 History of Gear Measurement - Measuring Machines and Traceability 1900-2005 - *Gear Product News Oct*.

[8] Frazer R C, Bicker R, Cox B, Harary H and Haertig F 2004 An International Comparison of Involute Gear Profile and Helix Measurement *Metrologia* **41** pp.12-16

[9] Haertig F, Keck C, Kniel K, Schwenke H I, Waeldele F and Wendt K 2005 A Novel Concept for High Accuracy Gear Calibration *Gear Technology* **22**(3) pp.16-20

[10] Haertig F, Keck C, Kniel K, Schwenke H I, Wendt K and Waeldele F 2003 Development of a Novel Gear Measuring Device of High Accuracy *Proc. of DECT'03 ASME 2003 (Chicago)* **22**(3) PTG-48105

[11] Mintrop H, and Beyer W 1961 Untersuchungen uber die Verwendbarkeit Von,, Angenaherten Evolventennormalen" zum Kalibrieren Von Evolventenprufgeraten *PTB-MITTEILUNGEN (Reprinted)* **71**(4) pp. 255-263

[12] Takeoka F, Komori M, Kubo A, Fujio H, Taniyama S, Ito T, Takatsuji T, Osawa S and Sato O 2007 Design of Laser Interferometric Measuring Device of Involute Profile *J. of Mechanical Design* **130**(5) pp.052602

[13] ISO, 1995, “Cylindrical gears -- ISO system of accuracy -- Part 1: Definitions and allowable values of deviations relevant to corresponding flanks of gear teeth,” 1328-1
[14] Physikalisch-Technische Bundesanstalt, Physikalisch-Technische Bundesanstalt brochure “Gear Metrology in the PTB“, *(Braunschweig, Germany)*

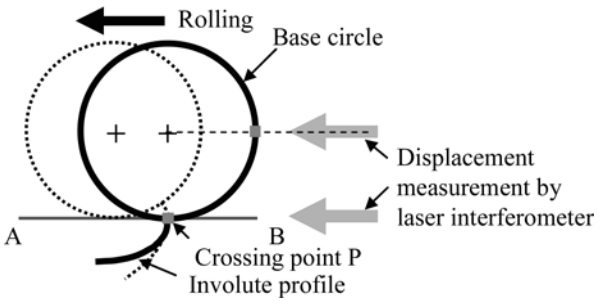

Figure 1. Measurement principle of involute artefact [12].

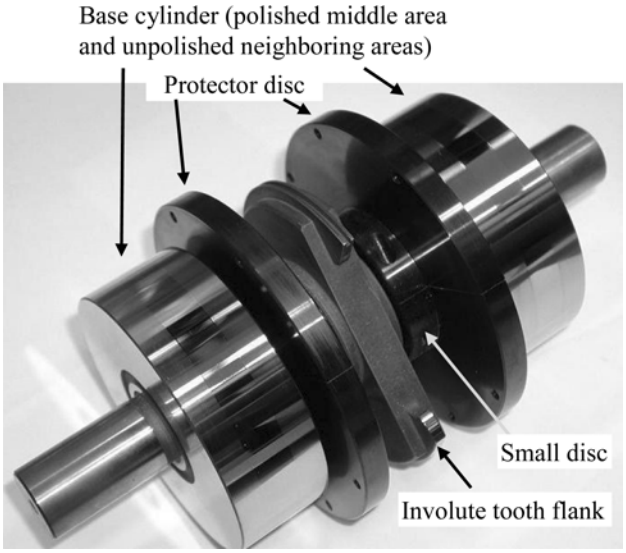

Figure 2. Involute artefact with base cylinder [12].

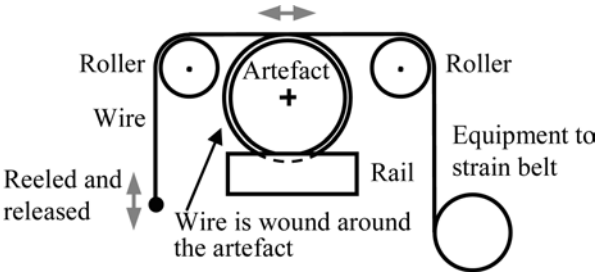

Figure 3. Driving system for involute artefact by PTB.

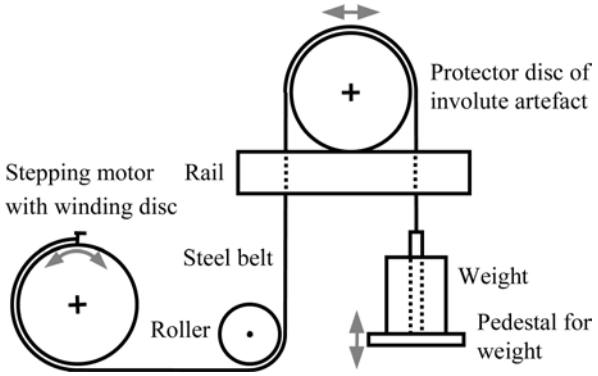

Figure 4. Wound-belt driving system for involute artefact [12].

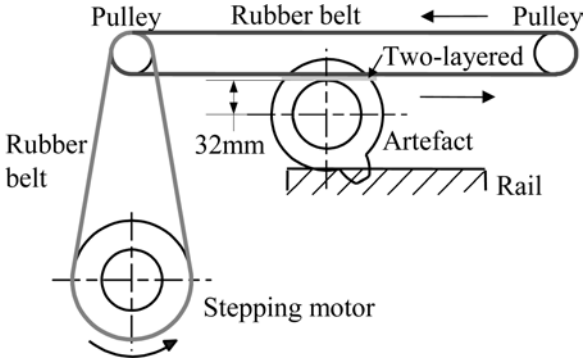

Figure 5. Nonslip driving system for involute artefact.

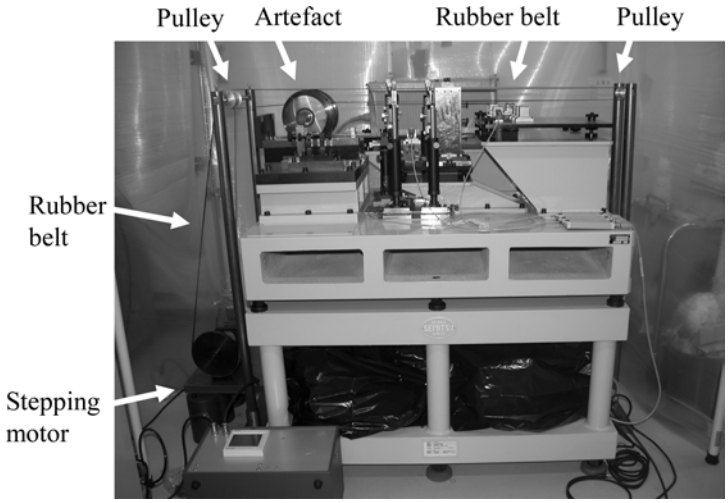

(a) Entire image of nonslip driving system

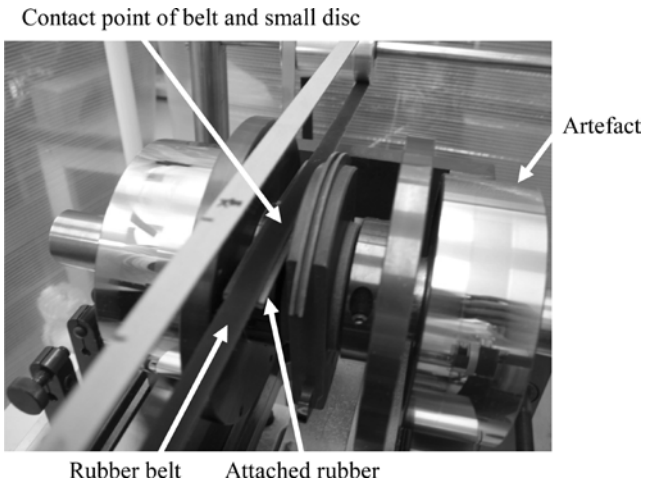

(b) Closeup of contacting point of belt and artefact

Figure 6. Photos of nonslip driving system.

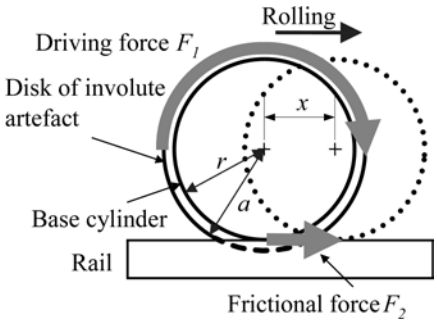

Figure 7. Simplified model for involute artefact driven by wound-belt driving system.

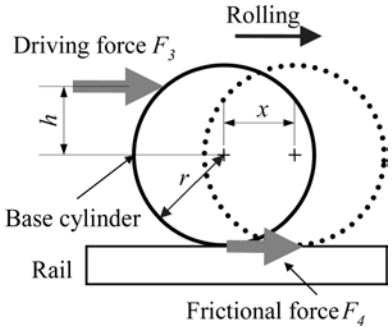

Figure 8. Simplified model for involute artefact driven by nonslip driving method.

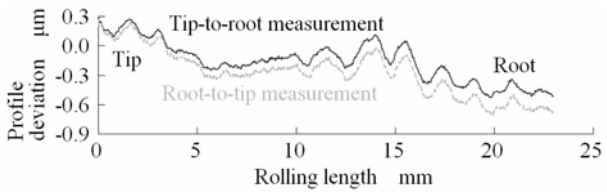

Figure 9. Mean curve of 10 measurement data for different measurement directions using wound-belt driving system (driving frequency: 100 Hz).

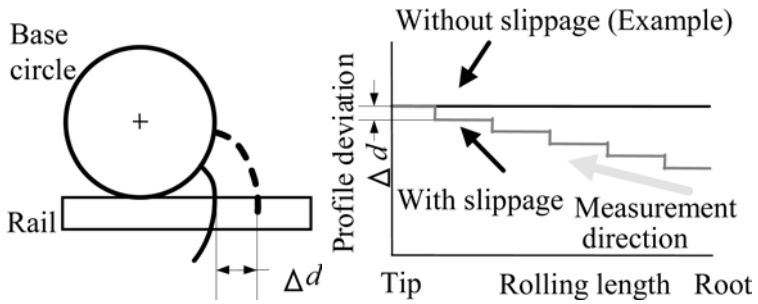

(a) Slipping condition (rotation without lateral motion) (b) Effect on measured profile deviation curve

Figure 10. Effect of slippage between artefact and rail, where artefact is measured from root to tip.

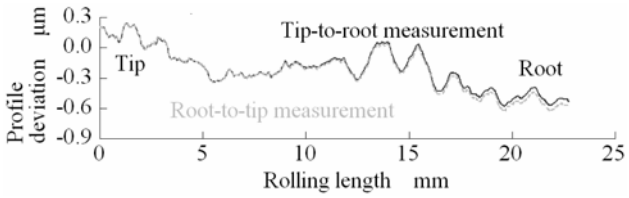

Figure 11. Mean curve of 10 measurement data for different measurement directions using nonslip driving system (driving frequency: 100 Hz).

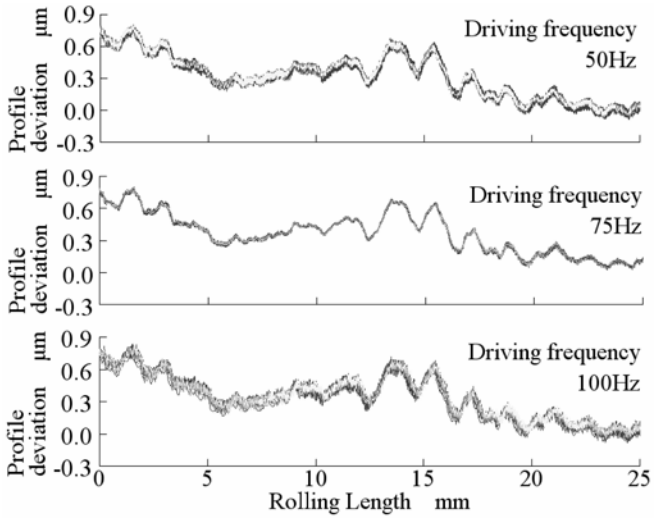

Figure 12. Profile deviation curves of 10 measurements in tip-to-root measurement at different driving frequencies of stepping motor using wound-belt driving system [12].

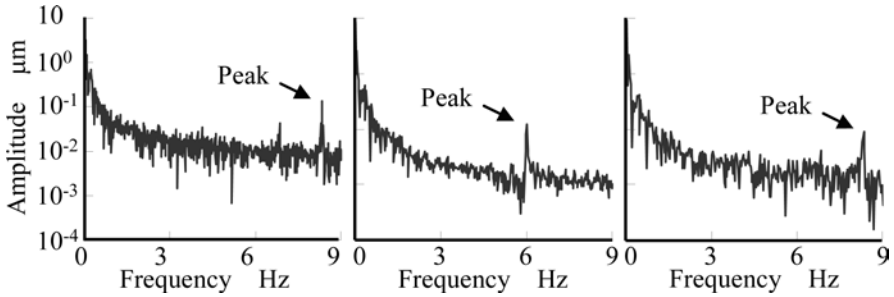

(a) Driving frequency of 50 Hz (b) 75 Hz (c) 100 Hz

Figure 13. Result of discrete Fourier transformation of measured profile deviation curve using wound-belt driving system [12].

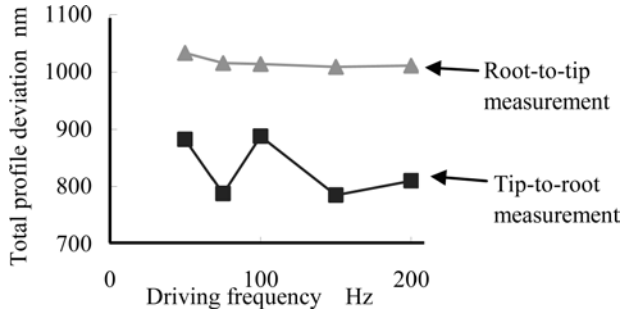

(a) Average

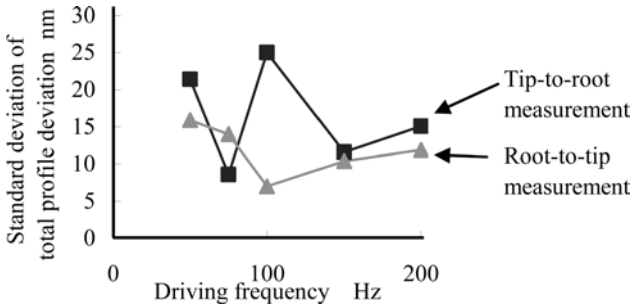

(b) Standard deviation

Figure 14. Total profile deviation at different driving frequencies using wound-belt driving system.

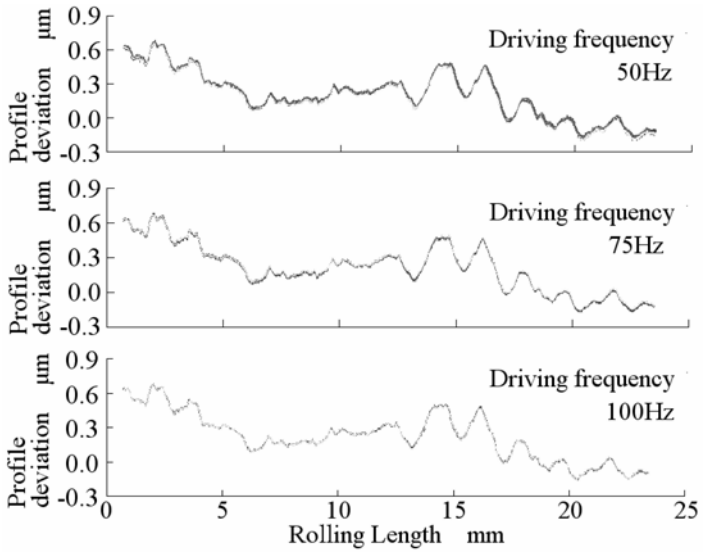

Figure 15. Profile deviation curves of 10 measurements obtained using nonslip driving system (tip-to-root measurement).

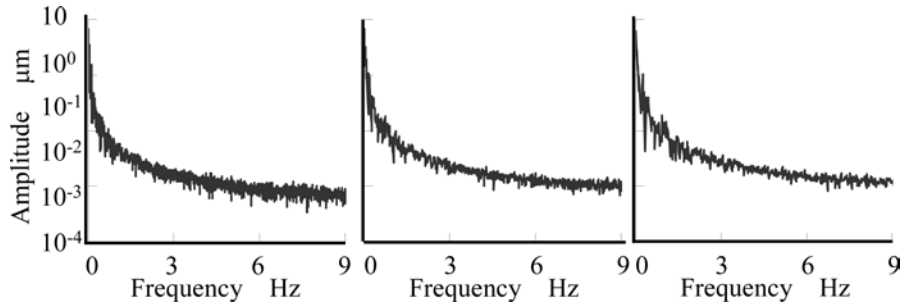

(a) Driving frequency of 50 Hz (b) 75 Hz (c) 100 Hz

Figure 16. Result of discrete Fourier transformation of measured profile deviation curve obtained using nonslip driving method.

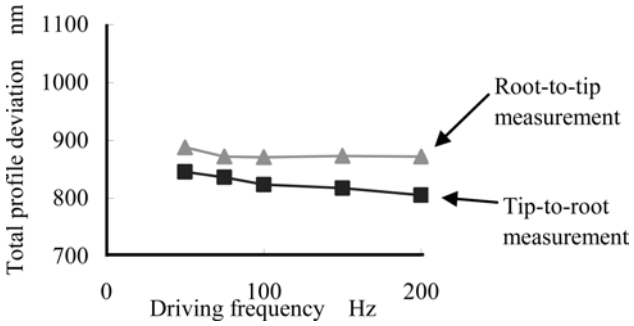

(a) Average

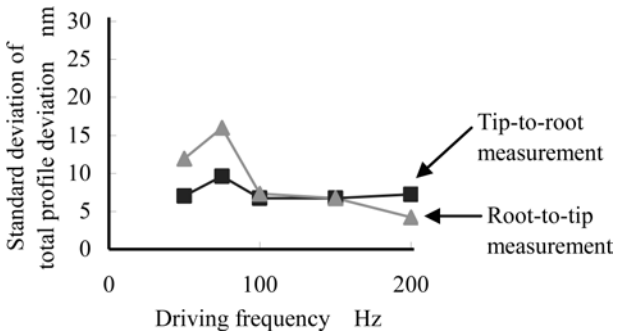

(b) Standard deviation

Figure 17. Total profile deviation at different driving frequencies obtained using nonslip driving system.

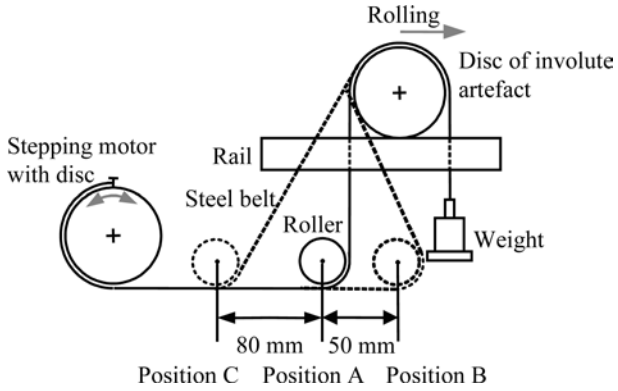

Figure 18. Position of roller of driving system.

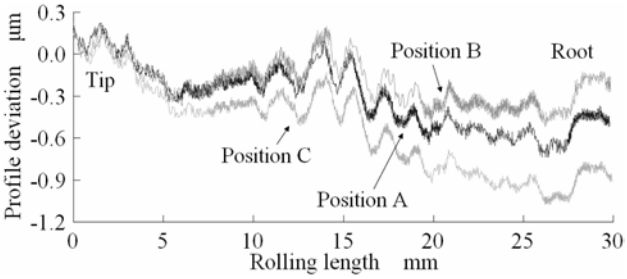

Figure 19. Measured profile deviations of involute artefact for different roller positions using wound-belt driving system

(driving frequency: 100 Hz, tip-to-root measurement).

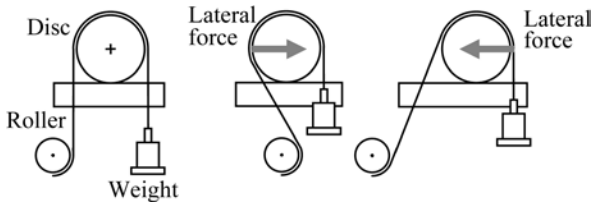

(a) Position A (b) Position B (c) Position C

Figure 20. Lateral force applied to artefact at each roller position.

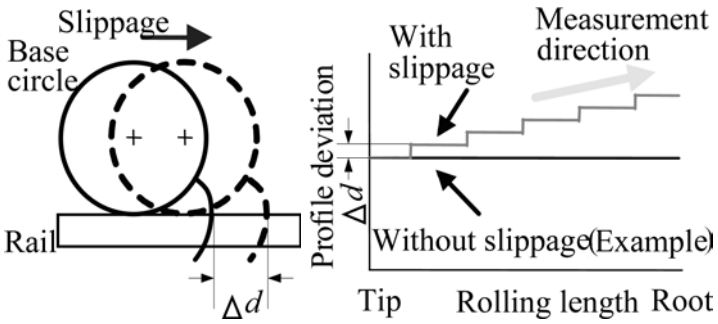

(a) Slipping condition (b) Effect on measured profile deviation curve

Figure 21. Effect of slippage between artefact and rail, where artefact is measured from tip to root as example.

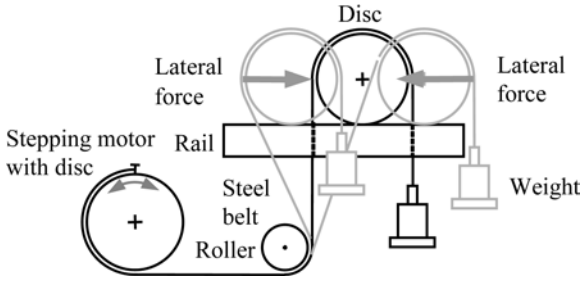

Figure 22. Lateral force applied to artefact during measurement under position A.

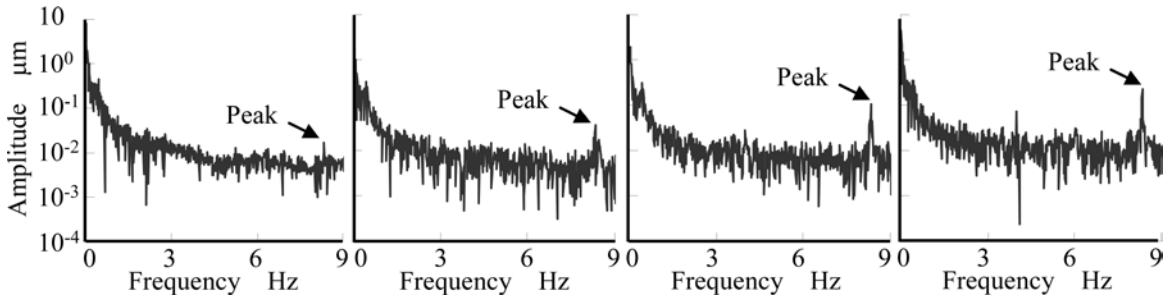

(a) 0.0 kg (b) 0.5 kg (c) 1.0 kg (d) 2.0 kg

Figure 23. Result of discrete Fourier transformation of measured profile deviation curve driven with different weights using wound-belt driving system (driving frequency: 100 Hz, tip-to-root measurement).

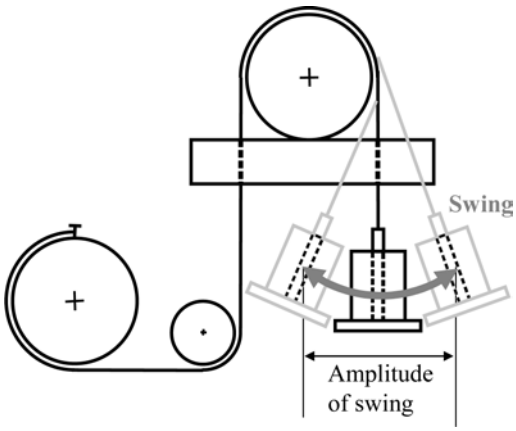

Figure 24. Observed swing of the weight

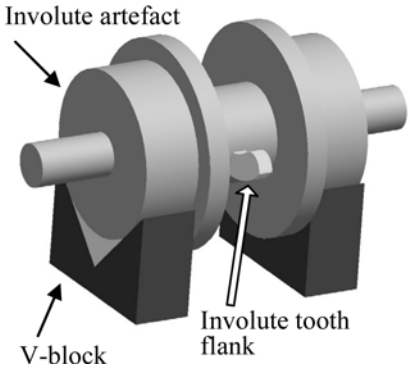

Figure 25. Setup of involute artefact for measurement using coordinate measuring machine.

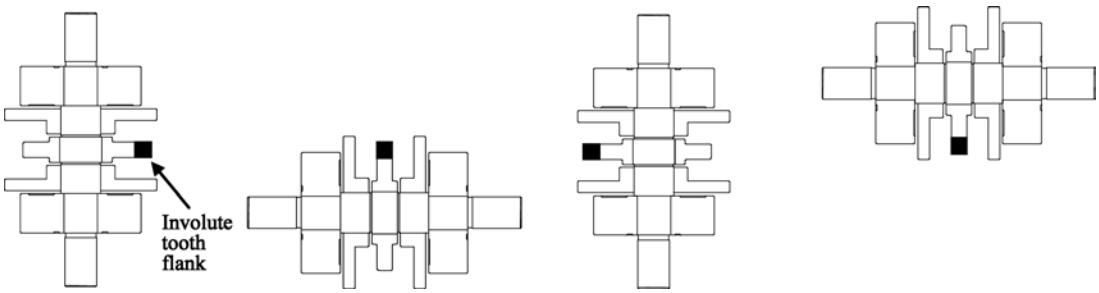

(a) Posture 1 (b) Posture 2 (c) Posture 3 (d) Posture 4

Figure 26. Four postures of involute artefact for measurement using coordinate measuring machine (view from above).

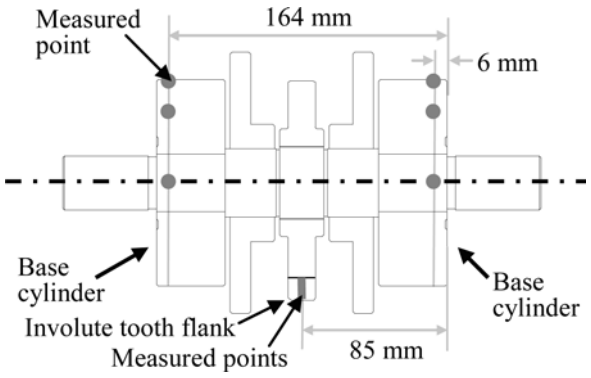

(a) Measured points on involute artefact

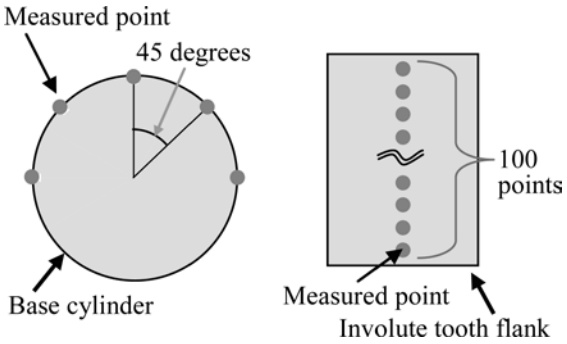

(b) Measured points on base cylinder (c) Measured points on involute tooth flank

Figure 27. Measured points on involute artefact using coordinate measuring machine.

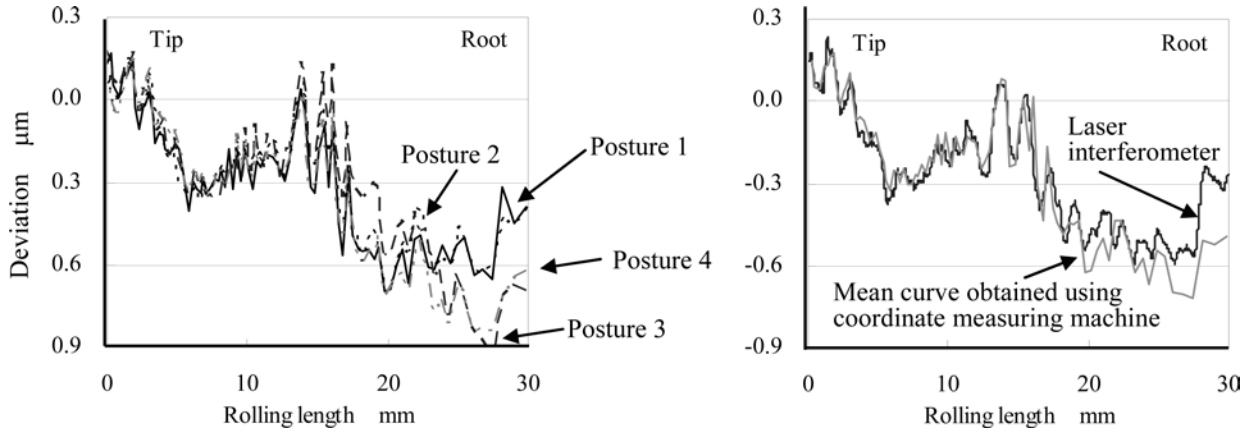

(a) Measurement results obtained using coordinate measuring machine at four postures

(b) Comparison between use of coordinate measuring machine and nonslip driving method.

Figure 28. Comparison between measurement results using coordinate measuring machine and nonslip driving method.

(a) Image of entire High Precision Gear Measuring Instrument (b) Closeup of measured involute artefact

Figure 29. Photo of High Precision Gear Measuring Instrument.

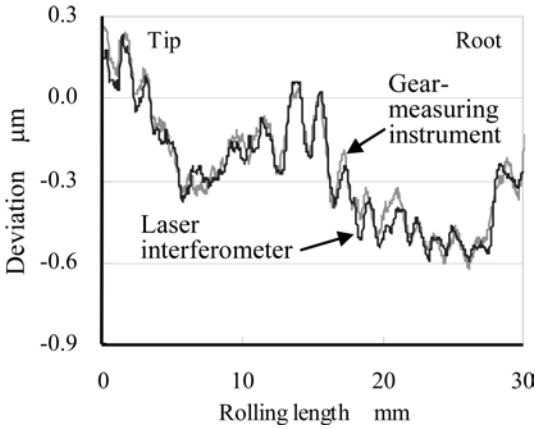

Figure 30. Measurement results obtained using gear-measuring instrument and nonslip driving method.